



Retrieving a common accumulation record from Greenland ice cores for the past 1800 years

K. K. Andersen,¹ P. D. Ditlevsen,¹ S. O. Rasmussen,¹ H. B. Clausen,¹ B. M. Vinther,¹ S. J. Johnsen,¹ and J. P. Steffensen¹

Received 13 October 2005; revised 18 February 2006; accepted 24 April 2006; published 10 August 2006.

[1] In the accumulation zone of the Greenland ice sheet the annual accumulation rate may be determined through identification of the annual cycle in the isotopic climate signal and other parameters that exhibit seasonal variations. On an annual basis the accumulation rate in different Greenland ice cores is highly variable, and the degree of correlation between accumulation series from different ice cores is low. However, when using multiyear averages of the different accumulation records, the correlation increases significantly. A statistical model has been developed to estimate the common climate signal in the different accumulation records through optimization of the ratio between the variance of the common signal and of the residual. Using this model, a common Greenland accumulation record for the past 1800 years has been extracted. The record shows significant 11.9 years periodicity. A sharp transition to very dry conditions is found just before A.D. 1200, and very dry conditions during the 13th century together with dry and cold spells during the 14th century may have put extra strain on the Norse population in Greenland and may have contributed to their extinction. Accumulation rates gradually decrease from a distinct maximum in A.D. 1394 to very dry conditions in the late 17th century and thus reflect the Little Ice Age.

Citation: Andersen, K. K., P. D. Ditlevsen, S. O. Rasmussen, H. B. Clausen, B. M. Vinther, S. J. Johnson, and J. P. Steffensen (2006), Retrieving a common accumulation record from Greenland ice cores for the past 1800 years, *J. Geophys. Res.*, *111*, D15106, doi:10.1029/2005JD006765.

1. Introduction

[2] The net precipitation rate in the accumulation zone of an ice sheet is recorded in the annual ice layer thickness profile which may be obtained from ice cores. However, due to local fluctuations and especially variations in the snow surface due to drift (sastrugies) the signal to noise variance ratio is rather poor, of the order 1–3, as established from comparisons of different shallow cores drilled close to one another [Fisher *et al.*, 1985]. The deep ice cores in Greenland are distributed mainly along the ice divide. As demonstrated by several authors these cores contain a common climatic signal over the large-scale climatic changes during the last glacial period [e.g., Johnsen *et al.*, 2001]. In order to separate the common climatic information from local phenomena and noise for the shorter-term variations during climatically stable periods it is however crucial to improve the signal-to-noise ratio. Crüger *et al.* [2004] showed that it is problematic to assume a common signal in records from different sites on the Greenland ice sheet on short timescales, but we expect extreme features and long-term variations to be concurrent over large parts of Greenland.

2. Ice Cores and Ice Flow

[3] In this work we compare the annual ice layer thickness profiles from five Greenland ice cores. The cores were chosen to ensure relatively long accumulation records of annual resolution over a common time period. The cores used in this study are the DYE-3 [Dansgaard *et al.*, 1982], the Milcent [Hammer *et al.*, 1978], the Crte [Hammer *et al.*, 1980], the GRIP [Johnsen *et al.*, 1992] and the NorthGRIP (NGRIP) [Johnsen *et al.*, 2001; North Greenland Ice Core Project Members, 2004] ice cores (Figure 1). Details about the location, accumulation rates of the cores and the length of the stratigraphies used for this study are given in Table 1. The NGRIP, GRIP and Crte ice cores are all located very close to the ice divide, GRIP and Crte in the center of the Greenland ice sheet and NGRIP 324 km NNW of the GRIP drill site. Milcent is in the central part of Greenland, but about 260 km west of the ice divide, whereas the DYE-3 drill site is located on the southern part of the ice sheet, about 30 km east of the ice divide. The ice cores used for this study are thus rather widely spaced, and all sites are subject to local meteorological conditions. Moreover the cores derive from both sides of the ice divide, which is known to influence the recorded signal [Clausen *et al.*, 1988; Rogers *et al.*, 1998] as the sites are affected by different air masses. Nevertheless it is expected that to a first approximation these ice cores share a common climate signal on an annual to decadal scale, which we here wish to

¹Ice and Climate, Niels Bohr Institute, University of Copenhagen, Copenhagen, Denmark.

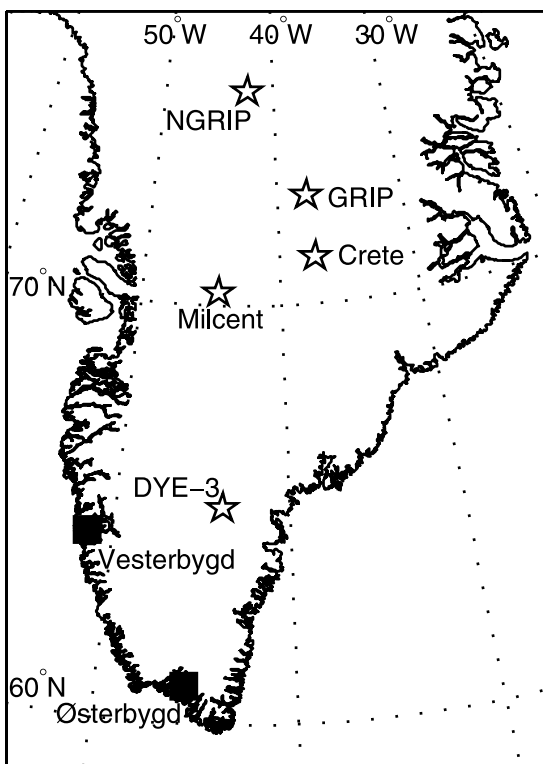


Figure 1. Location of sites in this study.

extract. The accumulation rates were determined by identifying and counting annual layers as determined from the high-resolution $\delta^{18}\text{O}$ and electrical conductivity measurement (ECM) records. In the case of NGRIP these records were supported by ion chromatographic (IC) measurements at 5 cm resolution over the upper 350 m [Vinther *et al.*, 2006]. The stratigraphy of the single cores has been cross checked using known volcanic horizons and ECM as also described by Vinther *et al.* [2006]. The dating uncertainty is estimated to be 1–2 years over the first millennium increasing to a few years at the end of the records used here.

[4] The stratigraphically dated records used in this study are of different lengths. The Crte and Milcent ice cores are intermediate length ice cores of about 400 m, and the length of the records presented is determined by the length of the cores. The DYE-3, GRIP and NGRIP ice cores are all deep ice cores reaching back through the last glacial period. The length of the used stratigraphies for NGRIP, GRIP and DYE-3 is given by the section where both high-resolution deconvoluted $\delta^{18}\text{O}$ and IC measurements provide reliable annual layer identification for the NGRIP ice core, and all three cores thus could be independently dated as part of the new “Greenland Ice Core Chronology 2005” (GICC05) [Vinther *et al.*, 2006]. The length of each stratigraphy is limited by the initial accumulation rate at the site determining the isotopic diffusion, together with the sampling resolution and the location of the brittle zone in the cores. The accumulation rate at the DYE-3 drilling site is high enough to preserve annual cycles in the isotopic signal throughout most of the Holocene. Hammer *et al.* [1986] used this fact to count annual layers continuously back to 5.9 ka BP and in sequences to about 8 ka BP. Vinther *et al.*

[2006] refined the isotopic measurements and completed the DYE-3 stratigraphy back to 8.2 kyr BP. This together with the work of Rasmussen *et al.* [2006] comprises GICC05 throughout the Holocene period, combining and cross dating the best available measurements from the NGRIP, GRIP and DYE-3 records.

[5] In order to derive annual accumulation rates from the observed annual layer thicknesses, the data had to be corrected for densification and thinning of the ice layers due to ice flow. This was done by using a flow model [Johnsen and Dansgaard, 1992; Johnsen *et al.*, 1999] also accounting for firnification at the top of the ice. In this way we obtained cross-dated chronological time series of annual accumulation rates over the latest two millennia, with relative dating errors being at most a few years. The ice flow in the DYE-3 region is complicated by upstream surface undulations, and the obtained accumulation rate profile thus contains longer-term variations of nonclimatic origin [Reeh, 1989]. In order to remove these variations we have filtered the DYE-3 accumulation record with a Butterworth filter of order 3 with a cutoff frequency of 0.001 year^{-1} , eliminating the lowest-frequency variations. The Milcent site is also slightly affected by upstream effects and the accumulation record has been linearly detrended. The obtained accumulation records are shown as 5 year average values in Figure 2.

[6] The most commonly used climatic parameter obtained from Greenland ice cores is the $\delta^{18}\text{O}$ record, which is a proxy for the temperature at the location of formation of the precipitation. However as indicated by model simulations [e.g., Werner *et al.*, 2000] the $\delta^{18}\text{O}$ signal is modulated by the amount of precipitation formed at a given time and temperature. The amount of precipitation is thus in some aspects a more direct climate signal than $\delta^{18}\text{O}$. Across large-scale climatic changes, like the Dansgaard-Oeschger events, there is a clear correlation between $\delta^{18}\text{O}$ and accumulation rates [Dahl-Jensen *et al.*, 1993]. Kapsner *et al.* [1995] and Crüger *et al.* [2004] have however shown that both during the most recent Holocene and the transition out of the last glacial period atmospheric circulation had larger influence on accumulation than temperature. Figure 3 shows scatterplots of $\delta^{18}\text{O}$ versus the logarithm of the accumulation for the records used in this study. The $\delta^{18}\text{O}$ records of DYE-3 and Milcent have here been corrected in the same manner as the accumulation records. The correlations are rather weak, and thus confirm that different information may be obtained from the two records. As noted above the accumulation

Table 1. Location, Annual Accumulation Rate, and Time Span Covered by the Stratigraphically Dated Ice Cores Used for This Study^a

Ice Core	Position	Accumulation Rate, m (ice eq.)/yr	Year Drilled	Oldest Year Counted
NGRIP	75.10°N, 42.32°W	0.19	1996	A.D. 187
GRIP	72.58°N, 37.64°W	0.23	1993	
Crte	71.12°N, 37.32°W	0.30	1974	A.D. 552
Milcent	70.30°N, 44.55°W	0.53	1973	A.D. 1174
DYE-3	65.18°N, 43.83°W	0.56	1979	

^aApart from NGRIP these are the same cores that were used by Vinther *et al.* [2003]. The stratigraphic dating of the GRIP and DYE-3 cores has recently been extended over most of the Holocene [Vinther *et al.*, 2006], but we here use them over their common period with NGRIP, back to A.D. 187.

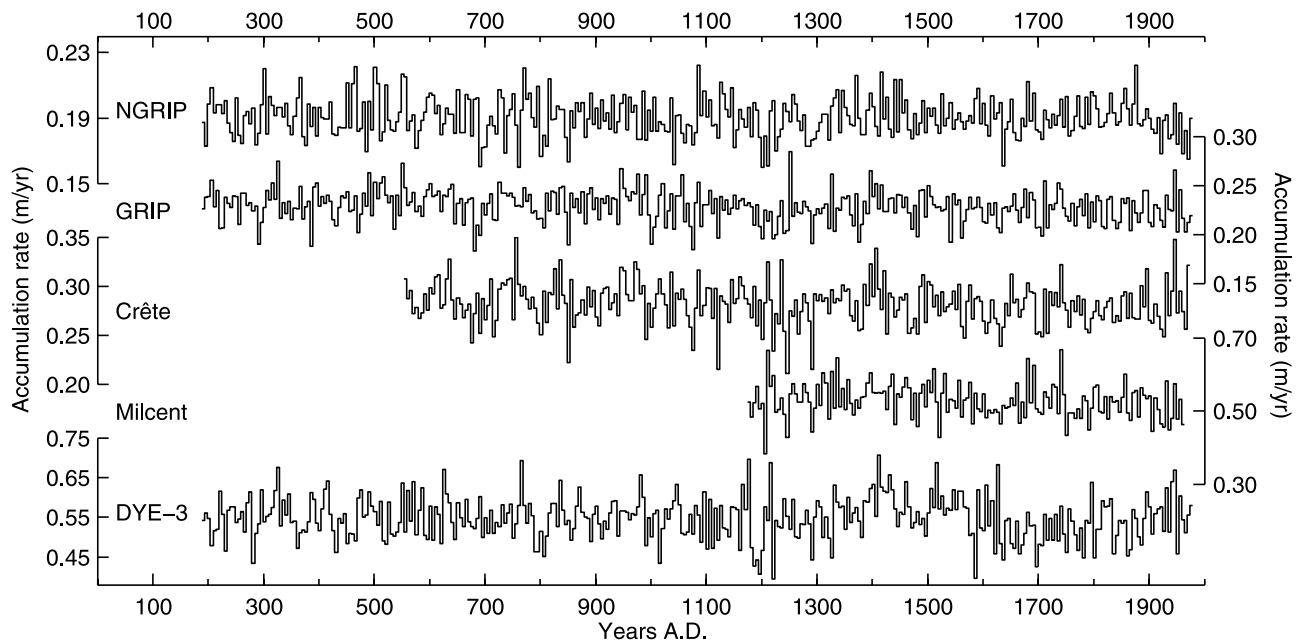


Figure 2. Flow-corrected accumulation series used in this work. The data are shown as 5 year average values.

records are probably strongly influenced by atmospheric circulation.

3. Statistical Distribution of Annual Layer Thicknesses

[7] The time series of annual accumulation rates obtained after correction for flow and compression are shown in Figure 2. It may be seen that the variance of each record roughly scales with the mean value (note the different axis scaling). This means that the amplitude of the local accumulation variability as well as the noise in a record is proportional to the mean accumulation rate. This fact is of importance for the model described here. The statistical distribution of annual layer thicknesses from each of the drill sites is shown in Figure 4. $\delta^{18}\text{O}$ sampling in the ice cores drilled in the 1970s (Crte, Milcent, and DYE-3) was done according to predicted timescales, such that 8 or 12 samples were cut per year. This means that the obtained accumulation rates from these cores take on discrete values, which is seen on the plots, especially for the shorter Crte and Milcent cores. The GRIP and NGRIP cores were cut in samples of constant size, and the discrete spectrum of layer thicknesses is changed into a continuous spectrum when correcting for the effect of layer thinning. The distributions of especially the longer cores are observed not to be symmetric around the mean. When plotted on a logarithmic accumulation axis the distributions become approximately symmetric, with a shape close to a normal distribution, as also observed by *Rasmussen et al.* [2006] for the accumulation record from the Early Holocene, Younger Dryas and Bølling sections of the NGRIP core. It may be expected that the accumulation rates follow Gamma distributions, as they are derived as the sum of positive independent precipitation events. Because of the discrete sampling rates and the limited number of annual layers in the records we can

however not distinguish between this and a lognormal distribution. In the following we will for simplicity use the fact that the logarithm of the accumulation rates is approximately normally distributed.

4. Noise Model

[8] From the set of available accumulation rate series we want to estimate a common accumulation record signifying

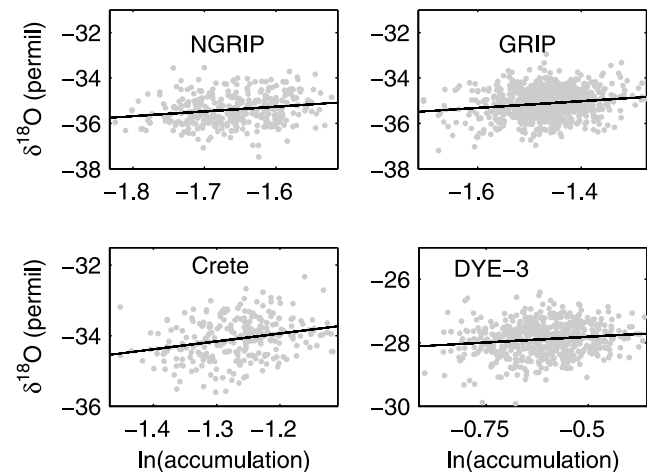


Figure 3. Scatterplots of the 5 year averaged logarithm of the accumulation rate and $\delta^{18}\text{O}$ for the whole length of the four longest series. The lines indicate the best linear fits to the data with slopes of 1.71, 1.83, 2.1, and 0.44 for NGRIP, GRIP, Crte, and DYE-3, respectively. The lower dependence for DYE-3 may be due to problems in the correction for ice flow. Correlations between $\ln(\text{accumulation})$ and $\delta^{18}\text{O}$ are 0.21, 0.17, 0.29, and 0.14, which are all significant at the 99% level.

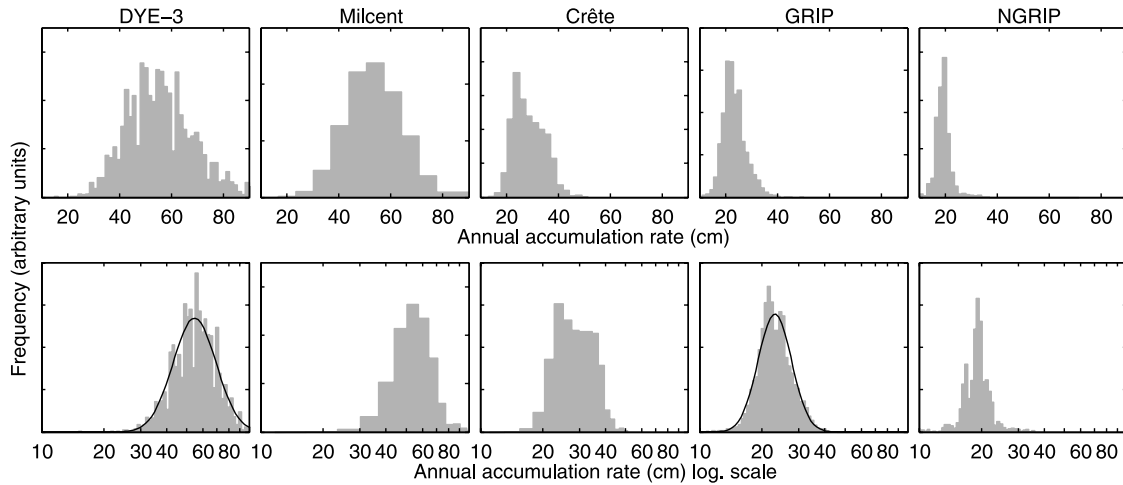


Figure 4. Distribution of annual accumulation rates. Discrete values of the accumulation rates are obvious, especially for the shorter Crête and Milcent cores but also for NGRIP, where a very high frequency is found around 19 cm. Distributions are plotted both on a linear and a logarithmic scale, and the distributions are seen to be more symmetric on the logarithmic scale. The distributions from the DYE-3 and GRIP records have been fitted to normal distributions on the logarithmic scale.

the variability in the mean regional precipitation over the past millennia. This signal is denoted $x(t)$. As pointed out by, for example, Fisher *et al.* [1985], the variance in the accumulation is ascribable to temporal, regional areal and local areal variability. We are here only interested in the common temporal variability. The local variability due to blowing snow and heterogenous snowfall is considerably diminished through temporal averaging over intervals of a few years. The regional areal variability may be ascribed to varying atmospheric circulation and storm tracks together with orography [Ohmura and Reeh, 1991; Dethloff *et al.*, 2002; Crüger *et al.*, 2004].

4.1. Model

[9] As a first approximation we can assume that the measured accumulation at site i , denoted $x_i(t)$, receives a contribution from the common signal $x(t)$ with some site specific scaling constant α_i . In addition, $x_i(t)$ may contain regional variability, but it is here treated as noise such that the measured signal is given as,

$$x_i(t) = \alpha_i x(t) + \sigma_i \eta_i(t). \quad (1)$$

[10] The residual $\eta_i(t)$ is assumed have zero mean and unit variance such that σ_i^2 is the variance of the residual term. Further we will assume that the residual terms at two different sites i and j are uncorrelated; $\langle \eta_i \eta_j \rangle = \delta_{ij}$, where $\langle \cdot \rangle$ represents the temporal mean. As shown above the measured accumulation rates x_i are lognormally distributed. The noise as defined here consists of two main contributions, the larger-scale variability from site to site, which as a first estimate can be regarded as white noise, and the glaciological noise which is blue noise for annually resolved records [Fisher *et al.*, 1985]. The blue noise may be ascribed to blowing snow (sastrugies) and discrete measurements sampling but it can efficiently be reduced by temporal averaging, and the assumption that $\eta_i(t)$ can be regarded as white

noise is thus reasonable if we use accumulation data averaged over intervals large enough to remove the blue noise characteristics of the glaciological noise.

[11] Even though we do not know to which extent $x(t)$ is a stationary stochastic process we will treat it as such and define the (unknown) signal variance,

$$\sigma^2 = \langle x^2 \rangle - \langle x \rangle^2. \quad (2)$$

4.2. Temporal Averaging

[12] After having corrected for layer thinning and snow compression the annual layer thickness is a measure of the accumulated precipitation including noise attributable to drifting snow.

[13] If the climate signal is auto correlated over times longer than the sampling time the noise can be reduced by temporal averaging of the signal. By doing that we of course lose information on the fluctuations of the climate signal on timescales faster than the averaging time. With only few noisy time series available some temporal averaging is however necessary in order to improve the signal to noise variance ratio. Consider two records $x_i(t)$ and $x_j(t)$ related according to (1). With $y_i \equiv x_i - \langle x_i \rangle$ and $y_j \equiv x_j - \langle x_j \rangle$ being the deviations from the average, the temporal average over any odd number m of points is,

$$\bar{y}_i(t) = \frac{1}{m} \sum_{k=-\mu}^{\mu} y_i(t+k), \quad \mu = (m-1)/2. \quad (3)$$

The covariance between the series is then given by:

$$\langle \bar{y}_i \bar{y}_j \rangle = \frac{1}{m^2} \sum_{k=-\mu}^{\mu} \sum_{l=-\mu}^{\mu} \langle y_i(t+k) y_j(t+l) \rangle. \quad (4)$$

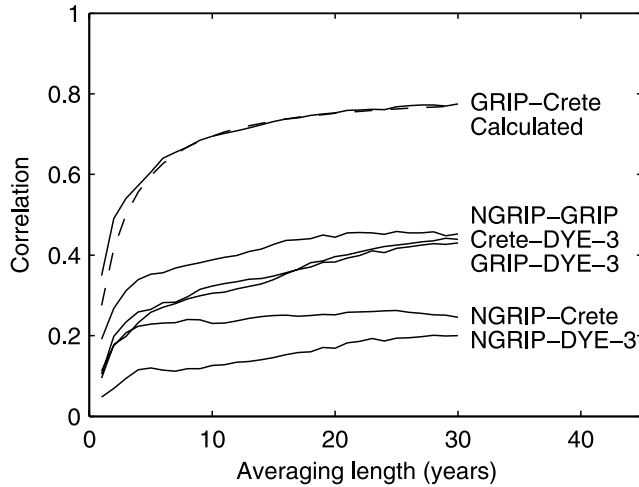


Figure 5. Correlation between the logarithm of the accumulation time series from the different ice cores. The correlation improves with averaging length as the noise decreases. The dashed line displays the correlation coefficient as calculated when using the estimated parameters for GRIP and Crte in (7) and assuming a correlation time of 10 years. The increase in correlation between the cores observed for averaging lengths below 5 years grows faster than for the theoretical result. This is probably due to the removal of blue noise, and an averaging time of 5 years was used in this work.

With the deviation from the climate signal being defined as $y = x - \langle x \rangle$ we have,

$$\begin{aligned} \langle y_i(t+k)y_j(t+l) \rangle &= \alpha_i \alpha_j \langle y(t+k)y(t+l) \rangle + \sigma_i^2 \delta_{ij} \delta_{kl} \\ &= \alpha_i \alpha_j c(k-l) + \sigma_i^2 \delta_{ij} \delta_{kl}, \end{aligned} \quad (5)$$

where we have introduced the autocovariance $c(\tau) = \langle y(t)y(t+\tau) \rangle$ for the climate signal. δ_{ij} is the Kronecker delta. By inserting this into (4) we obtain,

$$\begin{aligned} \langle \bar{y}_i \bar{y}_j \rangle &= \frac{1}{m} \alpha_i \alpha_j \left[c(0) + 2 \sum_{k=1}^{m-1} \frac{m-k}{m} c(k) + \frac{\sigma_i^2}{\alpha_i \alpha_j} \delta_{ij} \right] \\ &= \frac{1}{m} \alpha_i \alpha_j \left[I[c] + \frac{\sigma_i^2}{\alpha_i \alpha_j} \delta_{ij} \right], \end{aligned} \quad (6)$$

where $I(c) \equiv c(0) + 2 \sum_{k=1}^{m-1} c(k)(m-k)/m$. Finally we have the expression for the correlation coefficient,

$$\begin{aligned} C_{ij} &= \langle \bar{y}_i \bar{y}_j \rangle / \sqrt{\langle \bar{y}_i^2 \rangle \langle \bar{y}_j^2 \rangle} \\ &= \left[1 + \left(\frac{\sigma_i^2}{\alpha_i^2} + \frac{\sigma_j^2}{\alpha_j^2} \right) \frac{1}{I[c]} + \left(\frac{\sigma_i^2 \sigma_j^2}{\alpha_i^2 \alpha_j^2} \right) \frac{1}{I[c]^2} \right]^{-1/2}. \end{aligned} \quad (7)$$

[14] If the climate signal is assumed to be a red noise signal with autocorrelation $c(t) = \sigma^2 \exp(-|t|/T)$, where T is the correlation time, then by approximating the sum with an integral we obtain,

$$I[c] = 2\sigma^2 T \left[1 + \frac{T}{m} (\exp(-m/T) - 1) \right]. \quad (8)$$

[15] Figure 5 shows the correlation coefficients between all pairs of records used for this study, when averaging over an increasing number of years. On the basis of the findings in Section 3 the averages have been taken over the logarithm of the data. The maximum correlation of 0.77 is obtained between the GRIP and the Crte ice cores when averaging over 30 years. The correlations between the cores are generally significant at the 99% level, except for NGRIP-DYE-3 and NGRIP-Crte. The significance level for NGRIP-Crte is around 90%. A correlation time of about 10 years may be anticipated, and a comparison with the result obtained from (7) using $T = 10$ years agrees well with the ice core data for longer-term averages (dashed curve in Figure 5). For short-term averages the correlation coefficients between ice core records increase faster than the theoretical result of (7) in agreement with the blue noise spectrum observed by Fisher *et al.* [1985], while the curves mostly follow the shape of the theoretical result for averaging lengths above 3–5 years. We thus conclude that the major part of the blue noise has been removed when averaging over 5 year intervals, and apply this averaging approach in the rest of this work, assuming that the residual term $\eta_i(t)$ can be regarded as white noise.

5. Determination of Model Parameters

[16] With accumulation series from n ice cores we have to determine $2n + 1$ unknown parameters, namely (α_i, σ_i) for $i = 1, \dots, n$ and σ . The overall magnitude of the climate signal is arbitrary, and we set $\langle x \rangle = 1$. The variance of the climate signal (2) then becomes $\sigma^2 = \langle x^2 \rangle - 1$. Equations for the signal scaling parameters α_i may be estimated from averaging (1) over the whole length of the series,

$$\langle x_i \rangle = \alpha_i \langle x \rangle = \alpha_i. \quad (9)$$

Further equations can be derived from the covariance matrix. Assuming that the signals $x_i(t)$ are stationary processes the covariance c_{ij} between two signals may be calculated as

$$\begin{aligned} c_{ij} &= \langle x_i x_j \rangle = \langle (\alpha_i x + \sigma_i \eta_i)(\alpha_j x + \sigma_j \eta_j) \rangle \\ &= \alpha_i \alpha_j \langle x^2 \rangle + \sigma_i^2 \delta_{ij} \\ &= \alpha_i \alpha_j (\sigma^2 + 1) + \sigma_i^2 \delta_{ij}. \end{aligned} \quad (10)$$

[17] The set of equations from (9) and (10) is overdetermined and is solved by finding the set of estimated parameters $\tilde{\alpha}_i$, $\tilde{\sigma}_i$, and $\tilde{\sigma}$ that minimizes the total misfit M defined as

$$M = \sum_{i=1}^n (\tilde{\alpha}_i - \langle x_i \rangle)^2 + \sum_{i=1}^n \sum_{j=i}^n (\tilde{\alpha}_i \tilde{\alpha}_j (\tilde{\sigma}^2 + 1) + \tilde{\sigma}_i^2 \delta_{ij} - \langle x_i x_j \rangle)^2. \quad (11)$$

For the minimalization, the initial guesses were $\tilde{\alpha}_i = \langle x_i \rangle$, $\tilde{\sigma}_i = 0.8 \cdot \text{std}(x_i)$ and $\tilde{\sigma}^2 = 0.002$, but the estimated parameter values are insensitive to the choice of initial guesses, as long as reasonable values are used.

6. Optimal Climate Signal

[18] We now want to use the results of the presented model to calculate an estimate $\tilde{x}(t)$ of the common climate

Table 2. Values of α_i , σ_i , γ_i , and the Model Signal to Residual Variance Ratio, F_i , for the Five Records When Averaging Over 5 year Intervals for the Period A.D. 1176–1965

Ice Core	α_i	σ_i	γ_i	F_i
NGRIP	0.19	0.98e-2	0.333	1.68
GRIP	0.23	1.06e-2	0.337	1.82
Crte	0.28	1.45e-2	0.225	1.68
Milcent	0.53	3.49e-2	7.33e-2	1.42
DYE-3	0.54	5.43e-2	3.13e-2	1.18

signal $x(t)$ extracting maximum information on the common climate variability in the records. The method applied finds the linear combination of the individual records which optimizes the ratio between the variance of the common signal and the variance of the residual, as estimated from the model.

6.1. Accumulation Reconstruction

[19] On the basis of on the model given in (1), equations (9) and (10) may be combined to give the expression for the variance of any of the measured series x_i

$$\langle x_i^2 \rangle - \langle x_i \rangle^2 = \alpha_i^2 \sigma^2 + \sigma_i^2. \quad (12)$$

[20] With the presented model the ratio, F_i , between the total variance of a record and the variance of the residual is given as

$$F_i = \text{variance of record/variance of residual} = (\alpha_i \sigma / \sigma_i)^2 + 1. \quad (13)$$

[21] The estimate $\tilde{x}(t)$ of the common climate signal will be constructed such that the model based ratio between the variance of the total signal and the residual is maximized. The linear combination is expressed as

$$\tilde{x}(t) = \sum_i \gamma_i x_i, \quad (14)$$

with the coefficients γ_i being determined such that $\tilde{x}(t)$ represents $x(t)$ as closely as possible. We can do this in two different ways which lead to the same result. Firstly the linear combination which maximizes $F_{\tilde{x}}$ may be found directly. Combining (1) and (14) one gets $\tilde{x}(t) = \sum_i (\gamma_i \alpha_i x(t) + \gamma_i \sigma_i \eta_i(t))$. The signal to residual variance ratio $F_{\tilde{x}}$ for any linear combination of x_i values may be expressed as

$$F_{\tilde{x}} = \frac{(\sum_i \gamma_i \alpha_i)^2 \sigma^2}{\sum_i (\gamma_i \sigma_i)^2} + 1, \quad (15)$$

from which we have,

$$\frac{\partial F_{\tilde{x}}}{\partial \gamma_k} = \frac{2\sigma^2 \sum_i \gamma_i \alpha_i}{(\sum_i (\gamma_i \sigma_i)^2)^2} \left[\alpha_k \sum_j (\gamma_j \sigma_j)^2 - \gamma_k \sigma_k^2 \sum_j \gamma_j \alpha_j \right]. \quad (16)$$

By redefining $\tilde{\gamma}_j = \gamma_j \sigma_j^2 / \alpha_j$ we get,

$$\frac{\partial F_{\tilde{x}}}{\partial \gamma_k} = 0 \Rightarrow \sum_j (\tilde{\gamma}_j - \tilde{\gamma}_k) \left(\frac{\alpha_j}{\sigma_j} \right)^2 \tilde{\gamma}_j = 0, \quad (17)$$

with the solution $\tilde{\gamma}_j = \tilde{\gamma}$ for all j , where $\tilde{\gamma}$ is an arbitrary constant. From the definition above we thus get $\gamma_j = \alpha_j / \sigma_j^2$. As an alternative to maximizing the signal to residual variance ratio we can simply determine $\tilde{x}(t)$ by minimizing the root mean square error between a linear combination of the series $x_i(t)$ and (the unknown) $x(t)$. This results in the same linear combination as above. The estimated optimal climate record can thus be represented as,

$$\begin{aligned} \tilde{x}(t) &= \sum_i \left(\frac{\alpha_i}{\sigma_i^2} \right) x_i(t) \\ &= \sum_i \left(\left(\frac{\alpha_i}{\sigma_i} \right)^2 x(t) + \left(\frac{\alpha_i}{\sigma_i} \right) \eta_i(t) \right). \end{aligned} \quad (18)$$

[22] The estimated model parameters determined for the five ice core records over the common time interval, A.D. 1176–1965 are given in Table 2. The values for α_i found by the minimalization procedure agree well with the accumulation rates given in Table 1, although those are averages over recent years, whereas the α_i values correspond to long-term averages. As expected high σ_i values are found for the high accumulation sites. The model assumption that the residual signals are mutually uncorrelated was checked with the estimated series, and is largely confirmed. We find comparable modeled signal to residual variance ratios for all cores investigated here, meaning that the variability from all cores has comparable influence on the common signal. DYE-3 has the lowest ratio, which probably reflects the fact the DYE-3 is located east of the ice divide and considerably further south than the other ice cores included in this study. The DYE-3 site receives a larger proportion of its precipitation from cyclonic activity associated with the Icelandic low than the other cores [Hutterli *et al.*, 2005]. Moreover as mentioned earlier the DYE-3 accumulation record had to be corrected for ice flow at the site. When comparing the signal to residual ratios in this study with the signal-to-noise ratio estimates by Fisher *et al.* [1985] their values, especially for DYE-3, are considerably higher than what is found here (note that the definition of their ratios correspond to equation (13) minus 1). Fisher *et al.* [1985] in their study investigated the local signal to noise variance ratio by comparing the noise in a number of ice cores drilled close to another, whereas we here aim at the common signal over Greenland, considering everything else as the residual. The definition of noise in the two studies is thus inherently different and cannot readily be compared.

6.2. Sensitivity of the Reconstruction

[23] From the five cores we have calculated three estimates of the common accumulation curve as shown in Figure 6. The three curves are constructed by using the three, four, and five longest records over their common period, respectively. The three resulting curves show convincing agreement over their common periods, and all major minima and maxima recur in all curves. The correlation over the common interval is 0.94 between the reconstructions from three and four ice cores, 0.90 between the three and five cores reconstructions and 0.98 between the four and five cores reconstructions. The best agreement is thus found for the reconstructions with the most cores, but all three curves are highly correlated. We will in the following

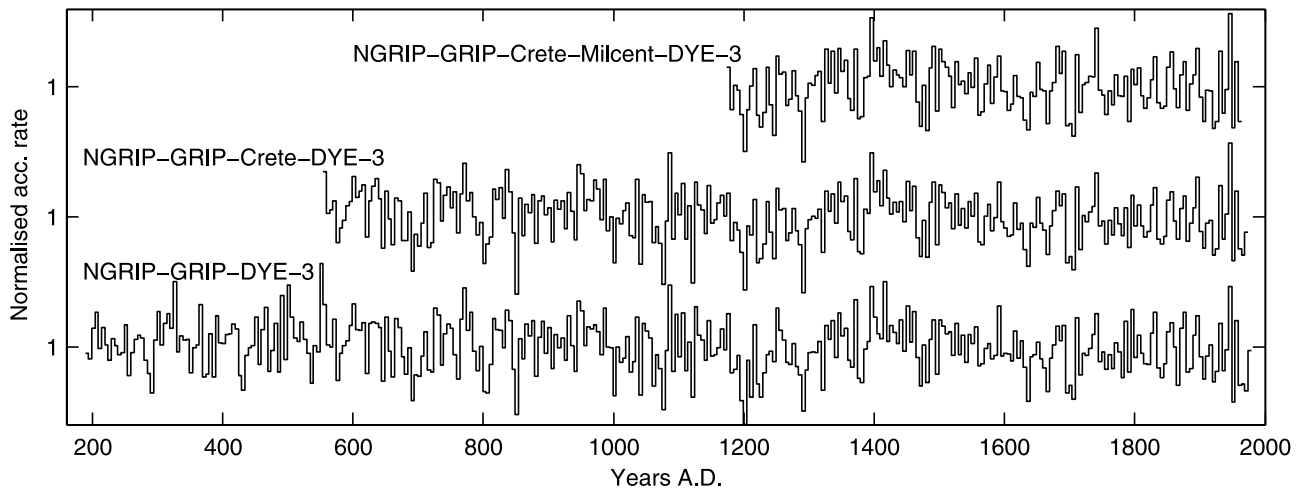


Figure 6. Optimal accumulation records based on three, four, and five cores, depending on the length of the records. The different reconstructions are highly correlated over the common interval A.D. 1178–1973.

discuss the longest record, based on NGRIP, GRIP and DYE-3 as a common accumulation rate reconstruction.

[24] When estimating the model parameters for the optimal climate curve, the original accumulation data are first averaged over discrete 5-year bins. These bins can of course be constructed in five different ways, and Figure 7 illustrates the variability associated with the choice of bins. Although differences are obvious, choosing a different set of bins does not significantly change the location of prominent maxima and minima.

6.3. Spectral Analysis

[25] Spectral analysis has been carried out on the longest reconstructed accumulation records with the five different

binings using the MTM method [Ghil *et al.*, 2002]. With 358 data points and three tapers a significance level of 99% has been used. Very little long-term variation is contained in the record, and significant peaks occur in the spectra of the single reconstructions with periods of 22.5, 20.4, 14–15, and 11.9 years. When averaging the spectra for the five different binings it may be seen that only the peak at 11.9 years is robust, whereas the peak around 14–15 years is weakly defined and only marginally significant (Figure 8). The sharp peak at 11.9 years could indicate a relationship with the 11-year sunspot cycle [e.g., Stuiver and Braziunas, 1993], however this could not be confirmed in a coherence analysis carried out with sunspot data covering the period A.D. 1700–1974 [Waldmeier, 1961] (data (updated to 2004) available

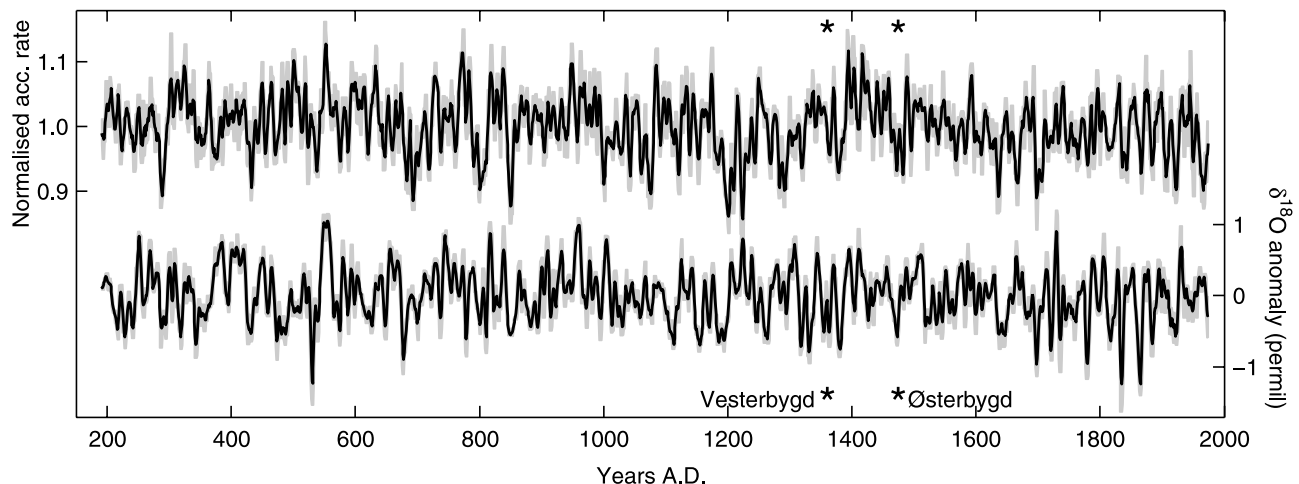


Figure 7. Optimal accumulation record over the period 191 A.D. to 1974 A.D. The curve has been constructed from the 5-year averaged accumulation records from DYE-3, GRIP, and NGRIP. For every year the curve shown here is the average value of the results obtained when using five different averaging bins. The highest and lowest values found for every year are indicated by the shaded envelope in order to illustrate the model variability associated with the different binning. The corresponding curve for the $\delta^{18}\text{O}$ records from the three sites is displayed below. The years A.D. 1360 and 1475 when the Norse settlements in Greenland were deserted have been marked on the plot.

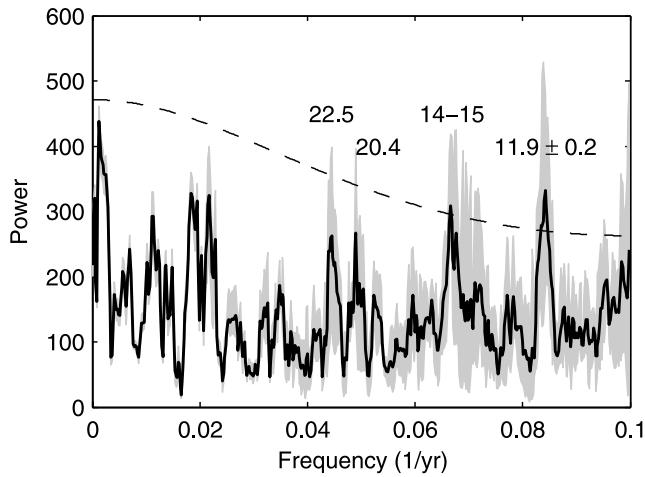


Figure 8. MTM spectral analysis of the longest reconstructions based on the NGRIP, GRIP, and DYE-3 records. The analysis has been carried out for all five possible binnings. The range of values obtained is shown as the shaded area, while the mean of the five spectra is shown as the solid line. The dashed line indicates the 99% significance level. The same major spectral peaks arise when using data averaged over 3 and 4 years wide bins.

from <ftp://ftp.ngdc.noaa.gov>). Further investigations of the possible connection between the accumulation record and solar forcing should be carried out, but are beyond the scope of this paper.

7. Other Reconstructions of a Common Accumulation Record

[26] In order to test the robustness of our results we also calculated a common accumulation record using several other methods. Besides the model presented in this paper we computed the simple stack of the available accumulation series, the “ α -stacked” series and the first principal component derived using the five accumulation records averaged over 5 years for the period A.D. 1176 to A.D. 1965.

7.1. Stacking the Records

[27] As an obvious choice the optimal record has been compared to a simple stack

$$x_s(t) = \frac{1}{n} \sum_i x_i(t) \quad (19)$$

of the original records. A probably more appropriate method is what we here call the “ α stack”,

$$x_{as}(t) = \frac{1}{n} \sum_i \frac{x_i(t)}{\alpha_i} \quad (20)$$

where all records are scaled down by their mean accumulation rate before stacking. As discussed here and by Fisher *et al.* [1985] the variance of individual accumulation records is approximately proportional to the average annual accumulation rate, which makes this approach very reasonable.

7.2. Principal Component Analysis

[28] A third comparison was made performing a principal component analysis (PCA) on the accumulation data. In the same way as for the other reconstructions the PCA analysis was performed on the 5 year logarithmically averaged accumulation data in order to avoid the blue noise. In analogy with the α stack each series was hereafter divided by its mean value, whereafter all series were centered around zero for the analysis, i.e., $z_i(t) = x(t) + (\sigma_i/\alpha_i)\eta_i(t) - 1$.

[29] Table 3 displays the weights on the first three EOFs. The first EOF carries 48% of the variance and is a strong signal of the common variance in the accumulation records. The weight of DYE-3 on EOF1 is strongest, and NGRIP is weakest. EOF2 carries 26% of the variance, and DYE-3 has strong negative weight on this pattern. DYE-3 has almost no weight on EOF3, which is most strongly influenced by NGRIP and Crte.

[30] The first principal component, PC1, is displayed in Figure 9 together with the records obtained by the accumulation, the stacking and the α stacking of the five ice core records averaged over 5 year bins for the period A.D. 1176 to A.D. 1965.

7.3. Evaluation of the Different Reconstructions

[31] The four different reconstructions displayed in Figure 9 are quite similar, and highly correlated with each other. However important differences may be noted. All reconstructions are formed as linear combinations of the five ice core records. The simple stacking puts equal weight on each record, whereas DYE-3 has strongest weight on PC1 as seen in Table 3. In the model presented in this work, and the α stack the coefficients in the linear combination are “corrected” for the accumulation rate, such that high accumulation records have lower coefficients (Table 2), which in fact prevents over representation of these records. This is also displayed by the fact that the correlation between the model reconstruction and the α stack is 0.96, whereas it is 0.89 and 0.87 for the correlation with the stack and PC1 respectively.

[32] On the basis of the model presented here (1) signal to residual variance ratios may be calculated for the different reconstruction approaches. The signal to residual variance ratio of the optimal record is $F_{\bar{x}} = \sum_i (\alpha_i/\sigma_i)^2 \sigma^2 + 1$, where the signal to residual variance ratios of the individual records are $F_i = (\alpha_i/\sigma_i)^2 \sigma^2 + 1$. Stacking the n records, $x_s(t) = 1/n \sum_i x_i(t)$, gives the signal to residual variance ratio, $F_s = \sum_i \alpha_i^2 / \sum_i \sigma_i^2 \sigma^2 + 1$, and the α stack results in a signal to residual variance ratio $F_{as} = N^2 \sigma^2 / \sum_i (\sigma_i/\alpha_i)^2 + 1$.

Table 3. First Three EOFs Based on the Five Accumulation Series Averaged Over 5 years for the Period A.D. 1176–1965^a

Ice core	EOF1	EOF2	EOF3
NGRIP	0.20	0.25	0.77
GRIP	0.40	0.28	-0.21
DYE-3	0.71	-0.69	0.08
Crte	0.37	0.33	-0.55
Milcent	0.40	0.53	0.20
Variance (%)	47.8	26.3	11.8

^aOn average, over the five possible sets of bins the carried variances are 46.9%, 27.2%, and 11.7%.

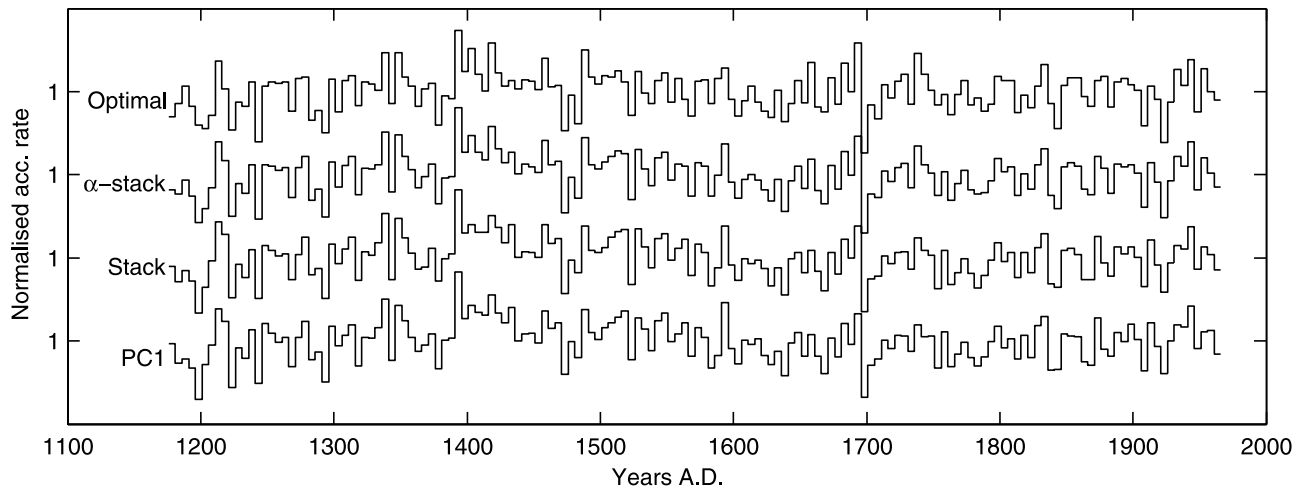


Figure 9. Resulting accumulation profiles over the period A.D. 1176–1965 using different methods as described in sections 6 and 7. The parameters and the signal to residual ratios calculated for the different climate series are given in Tables 2 and 4.

[33] As the principal components are linear combinations of the original data series the model signal to residual variance ratio may be calculated in the same manner as described in section 6.1. The series used for the PCA are $z_i(t) = x(t) + (\sigma_i/\alpha_i)\eta_i(t) - 1$, and the principal components are linear combinations $z_{pc} = \sum_i e_i z_i$ where e_i is the loading for z_i . This results in $F_{pc} = (\sum_i e_i)^2 \sigma^2 / \sum_i (\sigma_i e_i / \alpha_i)^2 + 1$.

[34] The estimated signal to residual variance ratios for the obtained reconstructions are given in Table 4. The model presented here gives significantly higher values than the other reconstructions, and α -stacking results in somewhat higher values than the principal component analysis and the simple stacking.

[35] From these evaluations we conclude that the model presented here gives a more representative reconstruction of the common signal than the other methods, and that it should be superior in reconstructing the common climate variability.

8. Climatic Interpretation of the Reconstruction

[36] On the basis of the analysis above the reconstructed accumulation record (Figure 7) is in the following discussed in terms of climate variability over the past 1800 years.

8.1. Accumulation and the Isotopic Climate Records

[37] The reconstructed accumulation curve is in Figure 7 displayed together with the corresponding $\delta^{18}O$ curve based on simple stacking of the individual records. As expected the two curves show only few similarities when compared over the past 1800 years. The correlation between the two is 0.31 which is significant at the 99% level and higher than for most of the individual records (see caption for Figure 3). There are several occurrences of coinciding minima in the two records. In the early part of the record this applies for the years A.D. 289 and A.D. 433. The very strong minimum for $\delta^{18}O$ in A.D. 530 is probably connected to a strong volcanic horizon in A.D. 529 [Vinther et al., 2006]. A minor minimum in accumulation is found in A.D. 537, and these two minima are followed by coinciding maxima in both curves around A.D. 551. Another strong minimum in $\delta^{18}O$

is found around A.D. 678, but the apparently corresponding minimum in accumulation is in fact not synchronous, it only occurs 15 years later, around A.D. 693.

[38] Over the latest centuries the common accumulation and $\delta^{18}O$ curves are characterized by concordant fast variations, which tend to be in phase. The correlation between the two curves increases to 0.41 for the period A.D. 1700 to 1974, and synchronous minima are found around 1697, 1778, 1833, 1861, 1884 and 1921 (Figure 10).

[39] All in all several occurrences of coinciding sharp minima and partly maxima are found over the 1800 years, but there is very little agreement in longer-term variations.

8.2. Climatic Implications of the Common Accumulation Record

[40] Focusing on the common accumulation record in Figure 7 some very interesting features may be noted. Several occurrences of very dry spells are found around A.D. 289, 433, 693, 801, 850, 1004, 1075, 1200, 1223, 1287, 1290, 1636, 1697, 1921, and 1965. Most of these are just dry spells of very short duration. However the period from A.D. 1004 to 1075 is generally arid with only a few years showing accumulation rates above average. This is followed by a moister century from A.D. 1081 to 1174. The

Table 4. Signal to Residual Variance Ratios for the Different Calculated Records and Ratios Between the Signal to Residual Variance Ratios for the Different Methods^a

	F
Model	3.7
α stack	2.9
Stack	2.1
PC1	2.2
F ratio	
$\frac{\text{Model}}{\alpha \text{ Stack}}$	1.2–1.4
$\frac{\text{Model}}{\text{Stack}}$	1.5–2.0
$\frac{\text{Model}}{\text{PC1}}$	1.4–2.0

^aThe values are averages of the five values obtained with different five year bin configurations.

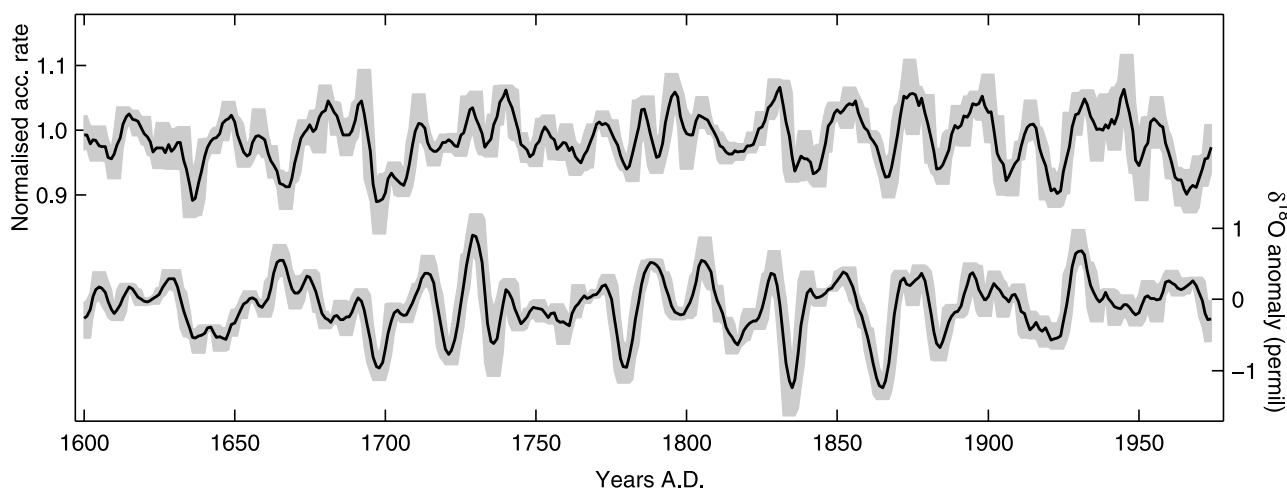


Figure 10. Same as Figure 7, but zoomed in on the latest centuries. Several coinciding minima between the two curves are found during this period.

13th century was generally drier than average, especially the earliest part around the strong minima in 1200 and 1223 with only a short moister spell around A.D. 1215. Significantly moister than average conditions are not encountered before the accumulation rate abruptly increases to the peak value in A.D. 1394. Following this sharp increase in accumulation rates conditions gradually become drier again until the three minima in A.D. 1636, 1667 and 1697 (see also Figure 10). After these minima the accumulation rate over the latest centuries shows distinct short time variability but no clear trend.

[41] The early part of the Greenland accumulation record presented here agrees well with findings from the Igaliku Fjord in the area of the Norse eastern settlement (Østerbygd) in southern Greenland (Figure 1). *Jensen et al.* [2004] using sediment cores from southern Greenland reported cold and moist climate condition between A.D. 500 and 700. In our record the period between the two minima in 433 and 693 is generally moister than average with only a few short dry spells. The Medieval Warm Period between A.D. 800 and 1250 is reported to have been very variable with generally increased wind stress in the Igaliku Fjord. A cooling event is reported in A.D. 960–1140. This time period encompasses the very dry 11th century in the accumulation record. After the accumulation maximum in A.D. 1174 our accumulation record shows two centuries of extremely low to low values. As already noted by [*Dansgaard et al.*, 1975] climate conditions in this period must have been harsh and put extra strain on the Greenland population. The 13th century shows three deep accumulation minima, beginning with the minimum at A.D. 1200. Each of these represents 5–10 year intervals with mean precipitation about 10% lower than the long-term mean. The mid-14th to early 15th century is the time when the Norse population disappeared in Greenland, and the Western Settlement (Vesterbygd) is believed to have lain waste around A.D. 1360 [*Lynnerup and Nørby*, 2004]. The last reports from the Eastern settlement (Østerbygd) are from a wedding in A.D. 1408, and it is believed to have been deserted around 1450–1500 as marked in Figure 7. The 14th century shows low $\delta^{18}\text{O}$ values with spells of dry conditions, most markedly around 1380 where both the accumulation and isotope records have a distinct minimum. After the abrupt

accumulation increase in A.D. 1394 short dry periods recurred in A.D. 1470–1480. Unusually dry periods may thus very well have contributed to the demise of the Norse population. The sustainability of pasture and livestock was marginal even under “normal conditions” [*McGovern*, 2000], and the Norse in the Eastern Settlement designed irrigation constructions directing water from high lakes into their fields. This laborious undertaking strongly indicates that precipitation and water supply was indeed critical for farming and grassing fields. The deep minimum in the record around A.D. 1200 also precedes a period where a shift toward a more marine diet (fish and seal) is observed [*Arneborg et al.*, 1999]. It is commonly assumed that the reason for the decline of the Norse settlements was the change to a colder climate in the Little Ice Age, however, this happened on a much longer timescale than the spells of very low precipitation. This means that we must expect that it was easier for Norse farmers to adapt to the change in temperature, and the drought could have initiated the Norse abandoning farming and their ultimate disappearance.

[42] A sharp increase in accumulation occurs just before the peak value in A.D. 1394, with some of the highest values recorded over the whole period. This sudden increase in accumulation coincides with the abrupt increase in sea-salt concentration in the GISP2 ice core [*Kreutz et al.*, 1997] interpreted as increased meridional atmospheric circulation intensity at the onset of the little ice age. In our reconstructed accumulation record, besides a shorter dry interval around A.D. 1470–1480, the accumulation rate slowly decreased until the second half of the 17th century, when minima of about 10% lower than average accumulation rates are found between 1636 to 1697. The Little Ice Age period may thus be seen as a minimum in accumulation during the period from 1635 to 1700 in the common accumulation record presented here. This minimum could possibly be associated with the Maunder minimum in A.D. 1650–1715 [*Stuiver and Braziunas*, 1993].

9. Summary and Conclusion

[43] A method has been presented to extract a common Greenland accumulation record over the past 1800 years.

Annual accumulation records contain blue noise attributable to depositional effects, and this noise may be diminished by temporal averaging over a few years. We here used accumulation rate records from five Greenland ice cores which have been very thoroughly cross dated. The common accumulation record was extracted by optimizing the ratio between the variance of the common signal and of the residual signal in all ice core records. The obtained signal has been compared to the stacked $\delta^{18}\text{O}$ record from the same cores, and besides episodic coinciding minima in both records very little agreement is found. The two records thus contain different climatic information and the accumulation record during this period is probably more related to atmospheric circulation changes than temperature variability.

[44] The obtained record of the common accumulation rate is quite robust with regard to the number of ice cores included in the reconstruction. Comparable reconstructions based on other methods were made. All records are highly correlated but the method presented here results in the highest signal to residual variance ratio, and thus is superior in reconstructing the common climate signal.

[45] The 1800 years accumulation record shows longer-term variations in accumulation rate over Greenland with especially the 13th and 14th centuries being persistently drier than normal, and with several very dry periods and a lack of unusually wet periods. This may very well have put additional strain on the Norse population in Greenland, and thus have contributed to their extinction.

[46] Spectral analysis of the record shows 11.9 years periodicity. This together with the low accumulation rates during the Maunder minimum indicates a possible solar influence which deserves further investigations.

[47] Although accumulation rates over Greenland are highly dependent on local and regional features it has been demonstrated that a common Greenland accumulation record may be extracted from very precisely dated records. The noise in the obtained climate signal has been minimized by temporal averaging, and the local contribution was separated by the optimization procedure. The obtained record should thus be a more valuable input to hemispheric and global-scale climate reconstructions than records from single ice cores.

[48] **Acknowledgments.** Discussions with David Fisher, Peter Thejll, and Jette Arneborg are greatly appreciated. K.K.A. was supported by the Danish National Science Foundation and the Carlsberg Foundation. This work is a contribution to the Copenhagen Ice Core Dating Initiative, which is supported by a grant from the Carlsberg Foundation. The reconstructed accumulation record is available from <http://icecores.dk>.

References

- Arneborg, J., J. Heinemeier, N. Lynnerup, H. L. Nielsen, N. Rud, and A. E. Sveinbjörnsdóttir (1999), Change of diet of the Greenland Vikings determined from stable carbon isotope analysis and ^{14}C dating of their bones, *Radiocarbon*, *41*(2), 157–168.
- Clausen, H. B., N. Gundestrup, S. J. Johnsen, R. Bindshadler, and J. Zwally (1988), Glaciological investigations in the Crte-area, central Greenland: A search for a new deep-drilling site, *Ann. Glaciol.*, *10*, 10–15.
- Crüger, T., H. Fischer, and H. von Storch (2004), What do accumulation records of single ice cores in Greenland represent?, *J. Geophys. Res.*, *109*, D21110, doi:10.1029/2004JD005014.
- Dahl-Jensen, D., S. J. Johnsen, C. U. Hammer, H. B. Clausen, and J. Jouzel (1993), Past accumulation rates derived from observed annual layers in the GRIP ice core from Summit, central Greenland, in *Ice in the Climate System*, NATO ASI Ser., Ser. I, vol. 12, edited by W. R. Peltier, pp. 517–532, Springer, New York.
- Dansgaard, W., S. J. Johnsen, N. Reeh, N. Gundestrup, H. B. Clausen, and C. U. Hammer (1975), Climatic changes, Norsemen and modern man, *Nature*, *255*, 24–28.
- Dansgaard, W., H. B. Clausen, N. Gundestrup, C. U. Hammer, S. J. Johnsen, P. M. Kristinsdóttir, and N. Reeh (1982), A new Greenland deep ice core, *Science*, *218*, 1273–1277.
- Dethloff, K., M. Schwager, J. H. Christensen, S. Kiilsholm, A. Rinke, W. Dorn, F. Jung-Rothenhusler, H. Fischer, S. Kipfstuhl, and H. Miller (2002), Recent Greenland accumulation estimated from regional climate model simulations and ice core analysis, *J. Clim.*, *15*(19), 2821–2832.
- Fisher, D. A., N. Reeh, and H. B. Clausen (1985), Stratigraphic noise in time series derived from ice cores, *Ann. Glaciol.*, *7*, 76–83.
- Ghil, M., R. M. Allen, M. D. Dettinger, K. Ide, D. Kondrashov, M. E. Mann, A. Robertson, Y. Tian, F. Varadi, and P. Yiou (2002), Advanced spectral methods for climatic time series, *Rev. Geophys.*, *40*(1), 1003, doi:10.1029/2000RG000092.
- Hammer, C. U., et al. (1978), Dating of Greenland ice cores by flow models, isotopes, volcanic debris, and continental dust, *J. Glaciol.*, *20*, 3–26.
- Hammer, C. U., H. B. Clausen, and W. Dansgaard (1980), Greenland ice sheet evidence of post-glacial volcanism and its climatic impact, *Nature*, *288*, 230–235.
- Hammer, C. U., H. B. Clausen, and H. Tauber (1986), Ice-core dating of the Pleistocene/Holocene boundary applied to a calibration of the ^{14}C time scale, *Radiocarbon*, *28*(2A), 284–291.
- Hutterli, M. A., C. C. Raible, and T. F. Stocker (2005), Reconstructing climate variability from Greenland ice sheet accumulation: An ERA40 study, *Geophys. Res. Lett.*, *32*, L23712, doi:10.1029/2005GL024745.
- Jensen, K. G., A. Kuijpers, N. Koç, and J. Heinemeier (2004), Diatom evidence of hydrographic changes and ice conditions in Igaliku Fjord, south Greenland, during the past 1500 years, *Holocene*, *14*(2), 152–164.
- Johnsen, S. J., and W. Dansgaard (1992), On flow model dating of stable isotope records from Greenland ice cores, in *The Last Deglaciation: Absolute and Radiocarbon Chronologies*, NATO ASI Ser., Ser. I, vol. 12, edited by E. Bard and W. S. Broecker, pp. 13–24, Springer, New York.
- Johnsen, S. J., H. B. Clausen, W. Dansgaard, K. Fuhrer, N. Gundestrup, C. U. Hammer, P. Iversen, J. Jouzel, B. Stauffer, and J. P. Steffensen (1992), Irregular glacial interstadials recorded in a new Greenland ice core, *Nature*, *359*, 311–313.
- Johnsen, S. J., H. B. Clausen, J. Jouzel, J. Schwander, A. E. Sveinbjörnsdóttir, and J. White (1999), Stable isotope records from Greenland deep ice cores: The climate signal and the role of diffusion, in *Ice Physics and the Natural Environment*, NATO ASI Ser., Ser. I, vol. 156, edited by J. S. Wettlaufer et al., pp. 89–107, Springer, New York.
- Johnsen, S. J., D. Dahl-Jensen, N. Gundestrup, J. P. Steffensen, H. B. Clausen, H. Miller, V. Masson-Delmotte, A. E. Sveinbjörnsdóttir, and J. White (2001), Oxygen isotope and palaeotemperature records from six Greenland ice-core stations: Camp Century, Dye-3, GRIP, GISP2, Renland and NorthGRIP, *J. Quat. Sci.*, *16*(4), 299–307.
- Kapsner, W. R., R. B. Alley, C. A. Shuman, S. Anandakrishnan, and P. M. Grootes (1995), Dominant influence of atmospheric circulation on snow accumulation in Greenland over the past 18,000 years, *Nature*, *373*, 52–54.
- Kreutz, K. J., P. A. Mayewski, L. D. Meeker, M. S. Twickler, S. I. Whitlow, and I. I. Pittalwala (1997), Bipolar changes in atmospheric circulation during the Little Ice Age, *Science*, *277*, 1294–1296.
- Lynnerup, N., and S. Nørby (2004), The Greenland Norse: Bones, graves, computers, and DNA, *Polar Rec.*, *40*(213), 107–111.
- McGovern, T. H. (2000), The demise of Norse Greenland, in *Vikings the North Atlantic Saga*, edited by W. W. Fitzhugh and E. I. Ward, pp. 327–339, Smithsonian Inst. Press, Washington, D. C.
- North Greenland Ice Core Project Members (2004), High resolution climate record of the Northern Hemisphere reaching into the last glacial interglacial period, *Nature*, *431*, 147–151.
- Ohmura, A., and N. Reeh (1991), New precipitation and accumulation maps for Greenland, *J. Glaciol.*, *37*, 140–148.
- Rasmussen, S. O., et al. (2006), A new Greenland ice core chronology for the last glacial termination, *J. Geophys. Res.*, *111*, D06102, doi:10.1029/2005JD006079.
- Reeh, N. (1989), Dating by ice flow modeling: A useful tool or an exercise in applied mathematics?, in *Dahlem Konferenzen: The Environmental Record in Glaciers and Ice Sheets*, edited by H. Oeschger and C. C. Langway Jr., pp. 141–159, John Wiley, Hoboken, N. J.
- Rogers, J. C., J. F. Bolzan, and V. A. Pohjola (1998), Atmospheric circulation variability associated with shallow-core seasonal isotopic extremes near Summit, Greenland, *J. Geophys. Res.*, *107*(D10), 11,205–11,219.

- Stuiver, M., and T. F. Braziunas (1993), Sun, ocean, climate and atmospheric $^{14}\text{CO}_2$: An evaluation of causal and spectral relationships, *Holocene*, *3*, 289–305.
- Vinther, B. M., S. J. Johnsen, K. K. Andersen, H. B. Clausen, and A. W. Hansen (2003), NAO signal recorded in stable isotopes of the Greenland ice cores, *Geophys. Res. Lett.*, *30*(7), 1387, doi:10.1029/2002GL016193.
- Vinther, B. M., et al. (2006), A synchronized dating of three Greenland ice cores throughout the Holocene, *J. Geophys. Res.*, *111*, D13102, doi:10.1029/2005JD006921.
- Waldmeier, M. (1961), The sunspot-activity in the years 1610–1960, Schulthess and Co AG, Zurich, Switzerland.
- Werner, M., U. Mikolajewicz, M. Heimann, and G. Hoffmann (2000), Borehole versus isotope temperatures in Greenland: Seasonality does matter, *Geophys. Res. Lett.*, *27*, 723–726.
-
- K. K. Andersen, H. B. Clausen, P. D. Ditlevsen, S. J. Johnsen, S. O. Rasmussen, J. P. Steffensen, and B. M. Vinther, Ice and Climate, Niels Bohr Institute, University of Copenhagen, Juliane Maries Vej 30, Copenhagen, 2100, Denmark. (kka@gfy.ku.dk)